Russian Chemical Reviews **73** (1) 25 – 36 (2004) © 2004 Russian Academy of Sciences and Turpion Ltd

DOI 10.1070/RC2004v073n01ABEH000867

Surface forces and physicochemistry of surface phenomena

N V Churaev

Contents

I. Surface forces 25
II. The influence of electrolytes, surfactants and polymers on the surface forces 28
III. Surface forces in wetting phenomena 32

Abstract. The results of modern theoretical and experimental studies of components of the long-range surface forces which determine the properties of dispersions and wetting liquid films are generalised. The bibliography includes 113 references.

I. Surface forces

During the last 10 – 15 years, numerous studies dealing with the interactions of interfaces through thin liquid films have been carried out as applied to colloids including nanoparticles and asymmetrical systems, *i.e.,* wetting films. This line of research forms the basis for solving a number of engineering problems such as control of the properties of dispersions, wetting, flotation and water treatment and the problems of environmental protection.

The physicochemistry of the surface phenomena considers the components of the surface forces and their change upon modification of the interfaces due to the adsorption of ions, surfactants and polymers including polyelectrolytes.

We shall start the discussion of the state-of-the-art of this field of physicochemical science with consideration of the results of fundamental studies of the surface forces which play the key role when the distances between the interacting particles or surfaces are comparable with the radius of action of these forces.

1. General remarks

Attractive or repulsive forces whose radius of action is much greater than the length of chemical bonds arise between condensed phases separated by a thin gas or liquid interlayer. The physical nature of such long-range forces can be different. They may be due to the electric fields of charged surfaces, fluctuating electromagnetic fields related to the movement of electrons in atoms and molecules, and structural forces arising upon the overlap of the boundary layers of the liquids with a changed structure.[1] The radius of action of these forces has the same order of magnitude as the correlation length in the liquid bulk (usually, this makes several nanometres). For solutions of polymers or surfactants, it is necessary, in addition, to take into account the steric forces which appear when the adsorption layers approach each other and overlap.[2]

N V Churaev Institute of Physical Chemistry, Russian Academy of Sciences, Leninsky prosp. 31, 119991 Moscow, Russian Federation. Fax (7-095) 952 53 08. Tel (7-095) 955 46 28

Received 3 July 2003
Uspekhi Khimii **73** (1) 26 – 38 (2004); translated by Z P Bobkova

The surface forces and the thermodynamic properties of thin liquid interlayers between two planar surfaces of solids are described conventionally by the disjoining pressure (Π), which was introduced by Derjaguin.[3] This value is equal to the difference between the pressure P acting on a planar liquid interlayer with thickness h and the pressure P_0 in the bulk of the same liquid outside the thin interlayer under equilibrium

$$\Pi = P - P_0 . \quad (1)$$

However, it should be borne in mind that the pressure Π does not always 'disjoin' the interlayer; depending on the direction of action of the surface forces, it can also attract the surfaces of different phases.

In the case of wetting films adjoining the gas phase, the P value in expression (1) is atmospheric pressure and the P_0 value characterises the pressure in the bulk region of the meniscus which is in equilibrium with the film.

The disjoining pressure $\Pi(h)$ is a very important thermodynamic parameter of the thin interlayer (film). Let us consider reversible changes in the state of the interlayer taking place upon the change in its thickness by ∂h, while the temperature T, the chemical potentials μ_i of the dissolved substances and the pressure P remain constant. As this takes place, the external forces which are necessary to ensure the equilibrium of the thin film do work equal to the increment of the Gibbs thermodynamic potential ∂G. Thus, it can be written that

$$\Pi(h) = -\left(\frac{\partial G}{\partial h}\right)_{T,P,\mu} . \quad (2)$$

The $\Pi(h)$ dependence which characterises the contribution of various components of the surface forces to the interaction of the surfaces is called the disjoining pressure isotherm. It contains full information on the state of the system at specified temperature, pressure and the composition of the bulk solution.

The surface forces are manifested first of all in disperse systems containing suspended particles that are involved in thermal Brownian motion. Upon the collision of particles, depending on the surface forces that act between them, the system can either remain stable, or alternatively, form weakly bound floccules or stable aggregates. Larger particles settle (or float to the surface) in a gravitational field to give porous precipitates whose structure depends on the forces that act between the particles.

In recent years, in view of a number of practical applications, special attention has been attracted by disperse systems with particle size of the order of several nanometres.

Wetting films, which model asymmetric systems, deserve special attention. These thin liquid films have the condensed

phase on one side and the phase of their own vapour or a different immiscible liquid on the other side.

The theory of several constituents of the surface forces has been developed in relation to a rather simple case of planar interlayers and films. Transition to calculations of the interaction of spherical (or other) particles is done using the Derjaguin approximation based on the integration of the local forces acting between the opposing 'planar elementary sections' of the curved surfaces.[4] For example, in this approximation, the force F that acts between two identical spherical particles with the radius r is given by

$$F = \pi r G(h), \tag{3}$$

where $G(h)$ is the free energy of interaction between planar interlayers with the thickness h,

$$G(h) = \int_h^\infty \Pi(h)\mathrm{d}h\,. \tag{4}$$

However, it should be borne in mind that the scope of applicability of the Derjaguin approximation is limited to interlayer thicknesses much smaller than the particle radius. Therefore, for calculation of the forces and energy for the interaction of particles smaller than 0.1 μm, more complex procedures are employed.[5–9]

2. Dispersion forces

The macroscopic theory of dispersion forces was first developed by Lifshits[10] for the simple case of attraction of identical planar surfaces in vacuum. Subsequently, it was extended to more complex systems in his joint work with Dzyaloshinsky and Pitaevsky.[11] The expression obtained for the disjoining pressure of thin interlayers ($h < 15$ nm) has the following form:

$$\Pi_\mathrm{m} = -\frac{A_{132}}{6\pi h^3}\,, \tag{5a}$$

where

$$A_{132} = \frac{3\hbar}{4\pi}\int_0^\infty \frac{(\varepsilon_1-\varepsilon_3)(\varepsilon_2-\varepsilon_3)}{(\varepsilon_1+\varepsilon_3)(\varepsilon_2+\varepsilon_3)}\mathrm{d}\xi. \tag{5b}$$

Here, the subscripts 1 and 2 refer to the phases that confine the thin film of liquid 3; $\hbar$ is Planck's constant. The frequency dependences of the dielectric constant of the medium $\varepsilon(\mathrm{i}\xi)$ are taken on an imaginary frequency axis.

A qualitatively equivalent solution was obtained earlier by Hamaker[12] in terms of a microscopic approach. Therefore, the constant A_{132} is still called the Hamaker constant, although calculation of this constant from Eqn (5b) gives a markedly different value.

For interlayers with a thickness of $>40-50$ nm, where the electromagnetic retardation effect, first taken into account by Casimir and Polder,[13] is manifested, the disjoining pressure decreases more sharply with an increase in the interlayer thickness h

$$\Pi_\mathrm{m} = -\frac{B}{h^4}\,. \tag{6}$$

In the case of dielectrics, the parameter B depends on the difference between the dielectric constants ε_0 of the interacting bodies and the interlayer separating them and amounts to $\sim 10^{-25}$ J m. For metals, the values of B are higher by approximately an order of magnitude.[1]

To calculate the dispersion forces for the intermediate range of distances, computer programmes are required.[14–17] In this case, the calculation gives the functions $A(h)$ rather than the Hamaker constants, which extends the scope of applicability of Eqn (5a).

Positive A and B values correspond to attractive forces, while negative values imply repulsive forces. The values of these constants and the functions $A(h)$ were reported in monographs[1,2] and in some papers (see, for example, Refs 18–20). In one study,[18] the functions $A(h)$ were calculated using corrected spectral data for water interlayers. Dagastine *et al.*[19] reported the A values for the dispersion attractive forces through water interlayers for a number of solids such as silicon, quartz, diamond, mica, TiO_2, MgO, Al_2O_3, CaF_2, LiF, NaCl, KBr and CdS. The values of A for some other inorganic materials were also documented.[20]

Various methods have been developed for experimental verification of the theory of dispersion forces; the methods make use of model objects such as lens–plane, sphere–sphere and crossed cylinders whose movement towards each other simulates the contact of dispersion particles.

The commercially manufactured instruments (for example, Mark) for direct measurement of the surface forces use glass cylinders crossed at an angle of 90° and coated by mica sheets.[21] The measurements give the dependences of F/R on the shortest distance H between the surfaces of the crossed cylinders with the radius R.

Direct verification of the theory of dispersion forces has been carried out only for the interaction of model bodies in vacuum through interlayers of gases and nonpolar liquids. In the case of aqueous solutions as interlayers, comparison with the theory is hampered because the results of measurements depend not only on the dispersion forces but also on electrostatic and structural forces.

In recent years, atomic force microscopy (AFM) has been used more and more often to study the surface forces. This method allows one to measure the forces between a rounded tip or a small spherical particle (5–10 μm) and a planar surface. The interaction force is found from the deformation of a planar cantilever spring with a test particle attached to the spring end. The number of publications devoted to the use of this method is rapidly increasing. However, it is used most often not merely to verify the theory of dispersion forces but in more complex cases where several components of surface forces act simultaneously, including electrostatic forces, which cover the longest distances.

3. Electrostatic forces

The theory of interaction of charged particles can now be considered as being well developed.[1,2,21] Solutions for the cases of a constant potential (ψ) or a constant charge (σ) of planar surfaces approaching each other have been obtained. Subsequently, the theory has been corrected because, as the surfaces approach each other, the potential-determining ions can be desorbed under the action of the electric field of the opposite surface. This effect, which has been called charge regulation, is often taken into account when analysing the results of direct measurements of electrostatic forces.[22]

The electrostatic repulsion forces between likely charged surfaces are often calculated using the approximation of small surface potentials. The disjoining pressure isotherm has the following form:

$$\Pi_\mathrm{e}(h) = (2\varepsilon\varepsilon_0\kappa^2\psi^2)\exp(-\kappa h), \tag{7}$$

where ε is the dielectric constant of the dispersion medium, ε_0 is the electric constant, κ is the reciprocal Debye radius depending on the ionic strength of the solution.

To pass to the interaction forces between identical particles, relation (1) is used. In the case of small particles where relation (1) is inapplicable, more complex solutions should be used.[5] A strict estimation of the electrostatic interaction requires taking into account other effects, namely, polarisation of the electric double layers (EDL) and the possible redistribution of the surface charge as the particles approach each other. The role of these nonequilibrium phenomena has been considered in a review.[23] The influence of the image forces on the ion distribution near a charged wall and the effects of ion correlation and the finite volume of ions on the electrostatic interaction have been analysed.[24]

However, direct AFM measurements of the electrostatic repulsion forces[25–27] showed that, except for the region of small

distances, rather good agreement is observed between the experimental data and simple solutions of the theory. At least, the calculated ζ-potentials (which are usually equivalent to the surface potentials ψ) are close to the values measured by independent methods. However, it has also been found by AFM [28] that the measured forces depend on the velocity (v) at which the tip moves towards the planar mica surface when $v > 10$ μm s^{-1}. The relaxation times of the EDL were roughly estimated as 5–6 ms. The nature of slow relaxation of the dense part of the EDL has been considered by Dukhin and Liklema.[29] This effect is especially pronounced for high rates of particle movement towards each other, for example, in the case of vigorous stirring or turbulent flow of the dispersion.

In a dispersion consisting of two types of particles which differ in the sign of the ψ-potential, the electrostatic forces become attractive forces, which results in so-called heterocoagulation.[1] If the particle potentials differ only in magnitude, the particles may repel at large distances. The sign of the electrostatic forces changes when they approach each other to the critical distance

$$h_c = \kappa^{-1} \ln \frac{\psi_1}{\psi_2},$$

where ψ_1 and ψ_2 are the potentials of the interlayer surfaces. Coagulation takes place after overcoming a potential barrier formed upon the mutual effect of the electrostatic and dispersion forces.

The publications devoted to the theory of heterocoagulation and the results of experimental studies of the stability of dispersions with a predominantly aqueous dispersion medium have been analysed.[30] The researchers noted an important role of heterocoagulation in the technology of disperse materials.

4. Structural forces

Even the first direct measurements of the forces acting between crossed mica-coated glass threads or cylinders showed that at a distance of $H < 2-3$ nm between the surfaces, the results deviate from the Derjaguin–Landau–Verwey–Overbeek (DLVO) theory, which takes into account only dispersion and electrostatic forces.

This is exemplified in Fig. 1, which shows the results of measurements of the dependence of the repulsive force F/R of molecularly smooth glass surfaces in a 1.1×10^{-2} M aqueous solution of NaCl on the shortest distance H between the surfaces.[31] Small glass plates several micrometers thick cut out of the wall of a rapidly blown bubble were coated with silver from the inside (to obtain the fringe pattern which serves for measuring the interlayer thickness) and attached to the surface of glass cylinders with the radius $R = 1$ cm. The continuous and dashed curves in Fig. 1 correspond to DLVO theory calculations in the constant charge and constant potential approximations, respectively. The experimental points in the region of interlayer thicknesses of $H < 3$ nm lie above the calculated curves, indicating an additional participation of structural repulsion forces. These forces arise upon the overlap of the structurally changed boundary layers of water that exist near the hydrophilic surface of glass. Qualitatively the same results were obtained for solutions of NaCl with other concentrations (10^{-3} and 10^{-1} mol litre^{-1}).[31]

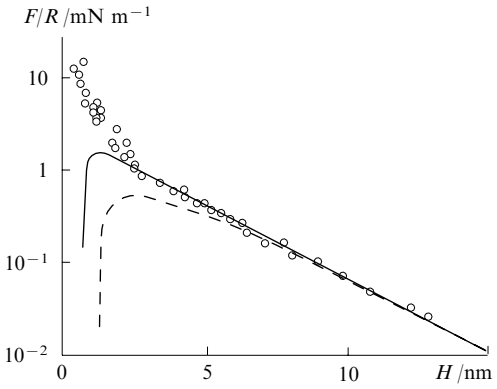


Figure 1. Dependences of the repulsion forces F/R on the distance H between smooth glass surfaces in a 1.1×10^{-2} M aqueous solution of NaCl.[31] For explanation, see the text.

The modified structure of the boundary layers of water was confirmed by a number of independent methods. For instance, recording of the IR spectra of water near the hydrophilic surface with the use of a laser excitation source [32] showed that water dipoles are oriented at a right angle to the surface. If the surface is charged, this orientation extends to 3–5 molecular layers.

It is known that near hydrophilic surfaces, the mobility of water molecules is retarded and the time of dielectric relaxation is an order of magnitude longer than that in the water bulk. Changes in the structure of the boundary layers of water are accompanied by strengthening of intermolecular bonds.[33]

Statistical mechanics calculations have shown that in aqueous solutions of electrolytes, the structural repulsion force between hydrophilic surfaces appears when the interlayer thickness is < 2 nm and increases exponentially as the interlayer becomes thinner.[34]

The experimental isotherms for the structural component of the disjoining pressure for water interlayers between the hydrophilic surfaces are approximated by the exponential dependence

$$\Pi_s(h) = K \exp\left(-\frac{h}{\lambda}\right), \tag{8}$$

where the parameter K describes the magnitude of the forces, and the parameter λ describes the long-range action. The parameters K and λ determined in experiments with thin interlayers of aqueous solutions between various hydrophilic surfaces can be found in monographs.[1, 21, 35]

The first attempts to develop a theory of structural forces were based on the Landau theory of second order phase transitions and the use of the order parameter η. This parameter was defined in such a way that it was zero in the isotropic bulk phase and nonzero (either a positive or a negative value) in the ordered phase. For small interlayer thicknesses, the calculations resulted in expression (8), where λ has the meaning of the correlation length and the parameter K, according to this approach, depends on the degree of surface ordering of water dipoles. The first estimates of these parameters were obtained in experiments with thin interlayers.[1] Subsequently, several versions of this approach have been used, including those taking into account the inhomogeneity of the orientational state of water molecules near the surfaces that confine the interlayer.[36, 37]

In a study devoted to the theory of structural forces,[38] the effects of excluded volume, dipole orientation, and the finite volume of water molecules were taken into account. This theory also predicts an exponential growth of structural forces with a decrease in the interlayer thickness. In addition, it was found that the period of oscillations of structural forces is close to the size of water molecules. The results of calculations are in good agreement with experimental data for a 10^{-3} M aqueous solution of KCl between mica surfaces.[21] The parameters K and λ for interlayers with a thickness of < 3 nm were found to be 3×10^6 N m^{-2} and 1 nm, respectively.

However, it should be borne in mind that the values of the parameters of structural forces presented here were obtained for hydrophilic molecularly smooth surfaces of glass and mica. Real surfaces are chemically heterogeneous and irregular and can be loosened or coated by adsorption layers of surfactants or polymers. Therefore, the quantitative determination of structural forces can only be used as rough estimates.

5. Hydrophobic forces

Some studies have shown that pronounced attractive forces act between the hydrophobic surfaces in water.[1,21,35] Their dependence on the interlayer thickness is described by the same equation (8), but the K values are negative in this case. The hydrophobic surfaces for measurements were usually produced by adsorption of a cationic surfactant or polyelectrolyte on glass or mica. It was found that hydrophobic forces have a greater radius of action than hydrophilic repulsion forces and the range of action increases with an increase in the degree of hydrophobicity of the surfaces. The measured λ values were 1 to 65 nm, depending on the experimental conditions.

The hydrophobic attraction detected in some cases when the distance between the surfaces is up to 100 nm is attenuated with a decrease in H according to a binomial exponential law with $\lambda = 13-15$ nm at long distances and with $\lambda = 1-2$ nm at short distances.

The physical nature of the hydrophobic attractive forces still remains unclear. Once it was assumed that this effect can be attributed, by analogy with the hydrophilic repulsion forces, to the structural changes of the boundary layers of water. Indeed, computations have shown[39,40] that the density of water decreases near a hydrophobic surface, unlike a hydrophilic one. However, the thickness of such boundary layers does not exceed 2–3 nm, which does not suffice to explain the observed long-range action.

It has been shown[41] that a correlation between hydrophobic attraction forces and the contact angles of water can be followed only at small distances. Due to the sharp increase in the attractive forces at short distances, no force oscillations, involved in the case of hydrophilic repulsion, can be detected experimentally.

Apparently, the long-range attraction is related to evolution of bubbles of the gas dissolved in water on the hydrophobic surfaces and the subsequent coalescence of the bubbles[42] or to thermal oscillations of the surfaces of such bubbles.[43,44] The role of the bubbles was confirmed, in particular, by the fact that the hydrophobic attraction forces decrease as water is being degassed.[45–47] Numerous nanobubbles were detected by atomic force microscopy on the quartz surface hydrophobised by octadecyltrichlorosilane.[48] It was concluded that the bubbles are formed before the contact of the tip of the atomic force microscope with the substrate. If the long-range hydrophobic attraction forces are caused by coalescence of the bubbles, their size should be 10–50 nm, which is consistent with experimental observations.

The solvophobic attraction of the surfaces coated by a film of amorphous Teflon with 0.5-nm high surface irregularities was observed not only in water but also in many organic liquids (except for n-alkanes and n-alkanols).[49] The results obtained are in line with the hypothesised formation of submicrometre air bubbles on the interacting surfaces.

The experimental values of the parameters K and λ present in Eqn (8) in the case of the hydrophobic forces for various objects have been summarised in a review.[42]

It can be assumed that the proper hydrophobic attraction exists only in degassed water, *i.e.*, in the absence of gas bubbles. Thus the nature of structural forces can be interpreted from a unified standpoint by relating them to changes in the structure of boundary layers — an increase in the water density and the normal orientation of dipoles in the case of hydrophilic repulsion forces and a density decrease and a tangential orientation of dipoles in the case of hydrophobic attraction forces. In any case, the λ values for hydrophilic and hydrophobic forces are similar and amount to 1–2 nm, which corresponds to the correlation length in the water bulk. This permits inclusion of both types of short-range structural forces in the overall isotherm of the disjoining pressure.

II. The influence of electrolytes, surfactants and polymers on the surface forces

1. Electrolytes

The effect of the electrolyte composition and concentration shows itself through a change in the surface charge as a result of both ion exchange and the change in the Debye radius

$$\kappa^{-1} = (\varepsilon\varepsilon_0 kT)^{1/2} (8\pi z^2 e^2 c)^{-1/2}, \qquad (9)$$

where k is the Boltzmann constant, z is the charge number, e is the charge of an electron, c is the concentration of the solution (in mol cm^{-3}).

It can be seen from Eqn (9) that with an increase in the electrolyte concentration, the Debye radius decreases and, according to Eqn (7), this reduces the range of action of the electrostatic forces. The repulsive forces also decrease, due to the more pronounced influence of the change in the κh in the exponential quantity on the disjoining pressure Π_e. The calculated repulsive forces may increase due to the increase in the charge and the potential ψ of the surfaces, but to only a limited extent, because Eqn (7) was derived with the assumption of small ψ.

Several mechanisms of formation of the surface charge are known. The most important of these are dissociation of the ionogenic surface groups and ion exchange. Therefore, the surface charge is controlled most often by varying the pH, the ionic composition, and the concentration of the solutions.

Usually, the surface charge and potential are determined experimentally. This is done most often using methods based on the measurement of the streaming potential of the solution in a slot or a capillary and on the measurement of the rate of electrophoresis of dispersion particles.

This is exemplified in Fig. 2, which shows the results of measurements of the ζ-potential in 50–150 μm thick planar cells formed by polished glass surfaces.[50] These data provide an idea of the range of possible variation of the surface charge of glass. The calculations were performed using the Smolukhovsky equation with the Dukhin correction for the surface conductivity.

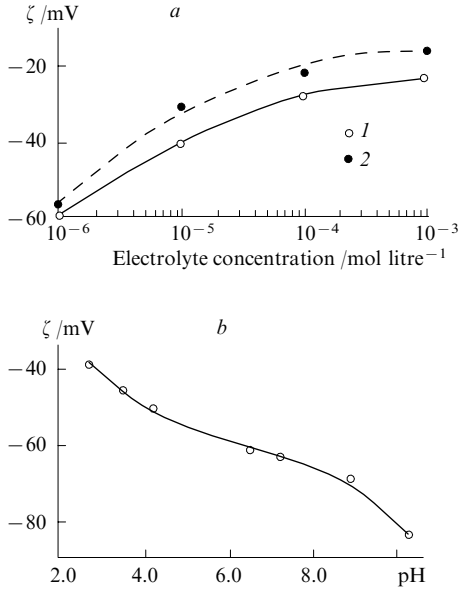


Figure 2. Dependences of the ζ-potential of the surface of glass plates[50] on the concentration of electrolytes (*a*) and on the pH (*b*).
Electrolyte: (*1*) NaCl, (*2*) $AlCl_3$

For quartz capillaries with molecularly smooth surfaces, the absolute values of the ζ-potential are much greater. This confirms the importance of the state of the surfaces, even if they are similar in chemical composition. In addition, the composition of the solution also plays a role. For example, at a constant ionic strength of a 10^{-3} M solution of KCl + HCl (or KOH), the ζ value at pH 10 reaches -140 mV, while at pH 2, it tends to zero.[51]

In the case of high surface potentials ($|\psi| > 100$ mV), electrostatic forces no longer depend on the surface charge and depend only on the electrolyte concentration and the κ^{-1} value.[52]

Atomic force microscopy measurements of the forces of interaction of the TiO_2 particles with a face of a rutile crystal in an electrolyte solution have shown [53] that for electrolyte concentrations of $< 10^{-2}$ mol litre^{-1}, the shielding length κ^{-1} is in good agreement with the value calculated from Eqn (9). At pH 5.6, only dispersion attraction forces corresponding to the Hamaker constant $A = 6 \times 10^{-20}$ J, close to the theoretical value, acted in the isoelectric point.

For spherical polystyrene particles with a diameter of 2 μm, long-range electrostatic repulsion was observed at KCl concentrations smaller than 10^{-2} mol litre^{-1} (see Ref. 54). For a 10^{-3} M solution, the experimental data were in good agreement with those calculated using the Derjaguin approximation (3) and the surface potential $\zeta_1 = 87$ mV was close to a value measured independently (83 mV).

In the interaction of a ZnS sphere of diameter 5 μm with a planar surface of mica with different ζ-potentials (-100 and -90 mV, respectively), the experimental dependence of the repulsive forces on the interlayer thickness was in better agreement with the condition of constant charge.[55] The researchers concluded that the solution of the Poisson – Boltzmann equation should be supplemented by a condition of charge control on both surfaces.

Dependences of the forces of interaction of spherical cellulose particles with a size of 20 – 30 μm on the distance H between them in aqueous solutions of electrolytes have been obtained by AFM.[56] These dependences were used to model some processes of the pulp-and-paper industry. In solutions with low concentrations of KBr (10^{-4} mol litre^{-1}), electrostatic repulsion is the main force at long distances; at $H < 20$ nm, steric repulsion predominates. With an increase in the pH, both forces grow due to an increase in the degree of ionisation of the COOH groups and swelling of cellulose. The observed dynamic effects were attributed to slow establishment of the equilibrium in the polymer – solution system.

Glass and fused quartz can swell in water, which gives rise to a surface gel layer.[57] Therefore, the results of measurements of surface forces can depend on the contact time between the surfaces and water. The diffusion structure of the surface layer can markedly decrease the Hamaker constant and complicate the calculation of electrostatic forces.

The surface roughness can also influence the attractive or repulsive forces. Comparative calculations were carried out for the case of interaction of a rough and a planar surface in a solution of a 1 – 1-electrolyte with ionic strength of 10^{-2} mol litre^{-1}. It was assumed that the ζ-potentials are 25 mV and the Hamaker constant is 10^{-20} J.[58] The roughness was specified by a random distribution of bulges and pits of a hemispherical shape and different radii. Roughness was found to influence substantially the shape of potential curves, especially for short distances between the surfaces. In particular, both the height of the potential barrier and the depth of the potential well can considerably decrease.

By direct microscopic examination,[59] stability of mixed dispersions of silica (SiO_2) and small crystals of NaCl in a saturated salt solution was detected; this cannot be explained in terms of the DLVO theory. The AFM measurements of interaction forces showed that short-range repulsive forces exist between a spherical silica particle and a planar surface of a NaCl crystal in a saturated solution of NaCl, whereas with KCl in place of NaCl, attractive forces appear. These effects were attributed to the action of structural (polar) forces caused by different orientation of the dipoles of water molecules.

2. Surfactants

Adsorption of ionogenic surfactants can change appreciably both the magnitude and the sign of the surface charge. For example, the initial negative charge of the quartz surface is strongly affected by adsorption of a cationic surfactant. Figure 3 shows the dependence of the ζ-potential on the concentration of the cetyltrimethylammonium bromide (CTAB) in a supporting electrolyte solution (5×10^{-4} mol litre^{-1} of NaCl) at pH 6.5 obtained by the streaming potential method. An increase in the content of CTAB results in charge reversal. When the surfactant concentration is close to the critical micelle concentration (CMC) (10^{-3} mol litre^{-1}), ζ-potential increases to $+140$ mV, and the surface charge increases to $+4$ μC cm^{-2} (see Ref. 60). On the basis of the two-layer adsorption theory,[61] it was shown that the adsorption potentials for the first and second layer of CTAB are $15\,kT$ and $11\,kT$, respectively. The curve in Fig. 3, plotted using the equations of this theory, is in satisfactory agreement with experimental data (dots).

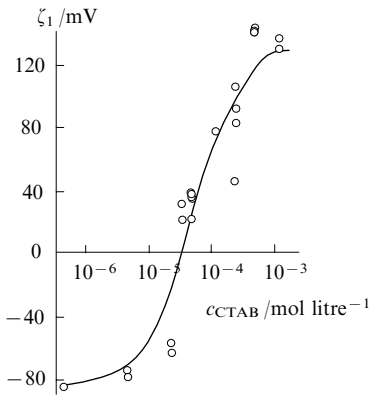


Figure 3. Results of measurements of the ζ_1-potentials of the surface of quartz capillaries for different concentrations of CTAB in a 5×10^{-4} M solution of NaCl (pH 6.5).[60] The curve corresponds to calculations in terms of two-layer adsorption.[61]

The same type of dependence of the surface charge on the surfactant concentration was obtained by direct measurements of the forces of interaction between mica surfaces in CTAB solutions.[62] When the CTAB concentration is low, electrostatic repulsion forces prevail over the dispersion attraction forces; upon neutralisation of the surface charge, the former are replaced by hydrophobic attraction forces.

It has been established [63] that the adsorption mechanism changes at pH 3 where no charged centres remain on the quartz surface. In this case, the bilayer adsorption of the surfactant becomes impossible. Processing of the resulting dependence of the charge on the CTAB concentration in terms of the monolayer adsorption model showed that the adsorption potential is $11\,kT$.

Subsequently, it has been found by AFM [64] that at a CTAB concentration higher than 2 CMC, cylindrical micelles are formed on the mica surface; over a period of 24 h, they are transformed into a planar bilayer structure.

In an alkaline medium, the formation of a second layer on the surface of glass takes place at a CTAB concentration below the CMC and the density of this layer is much lower than the density of the layer on the mica surface. By removing the second layer, it is possible to bring the glass surfaces in a tight hydrophobic contact.[65] The researchers cited suggested that the second layer

consists of separate bunches of surfactant molecules or surface aggregates.

Anionic surfactants influence the charge of the quartz surface into a much lesser extent. After the addition of 5×10^{-5} mol litre^{-1} of sodium dodecyl sulfate to the background solution of NaCl (10^{-4} mol litre^{-1}), the ζ-potential of the quartz surface slightly increased in magnitude (from -125 to -150 mV) and did not change upon further increase in the concentration of sodium dodecyl sulfate in the solution by an order of magnitude.[66]

The adsorption of nonionic surfactants on the hydrophilic surface up to the formation of a full monolayer leads to gradual hydrophobisation of the surface. The formation of the second layer in which the polar groups of the surfactant molecules are directed toward the solution makes the surface hydrophilic again. However, the ζ-potential does not change noticeably; its decrease has been noted only in the case of adsorption of nonionic surfactants whose molecules are capable of forming hydrogen bonds with the surface hydroxy groups.

Note that the influence of surfactant adsorption on the charge and hydrophilicity of the surface, which determine the electrostatic and structural forces, was analysed only for silicate surfaces; however, the key conclusions are valid at a qualitative level for the surfaces of other natural materials, because most of them are negatively charged.

3. Polymers

We shall start with a simpler case of noncharged polymers and then consider polyelectrolytes.

Nikologorskaya *et al.*[67] have employed dynamic light scattering to measure the Brownian diffusion coefficients of the particles of monodisperse silicasols Ludox-SM with the radius $r = 19$ nm and Syton-W50 ($r = 69$ nm) before and after the adsorption of polyethylene oxide (PEO) with a molecular mass of 4×10^4 and estimated the thickness of the adsorbed layers on the basis of the results obtained. At a low electrolyte concentration, the sols were stable due to the action of electrostatic repulsion forces. However, with an increase in the NaCl concentration to 10^{-2} mol litre^{-1} when the Debye radius became smaller than the length of the unfolded PEO molecule, flocculation of the sols took place in the presence of even small amounts of the polymer, as a result of binding of two particles to the same macromolecule (so-called bridging). As the PEO concentration increases and a filled adlayer is formed, the sols become stable once again due to the arising steric repulsion of the particles.

A study of the interaction of mica surfaces in aqueous solutions of ethylhydroxyethylcellulose showed[68] that the adsorbed macromolecules could be easily squeezed out of the interlayer space at 20 °C. This attests to a low adsorption energy. When the temperature was raised to 60 °C, the adsorption of the polymer increased, apparently due to a decrease in the hydrophilicity of the surface, and squeezing out of the molecules became difficult. Upon preliminary hydrophobisation of the mica surface, the adsorption of cellulose sharply increased and long-range steric repulsion was observed.

In aqueous solutions of a triblock copolymer (polyethylene oxide – polytetrahydrofuran – polyethylene oxide) with a molecular mass of 11 900 at a concentration below the CMC, steric repulsion force was detected between the surfaces of quartz spheres; the force increased monotonically as the spheres approached each other.[69] However, after long-term keeping of the spheres in a 10^{-4} % solution of the copolymer, thinning of the interlayer down to 10 nm gave rise to bridging bonds between the surface aggregates of the macromolecules. The steric repulsion was replaced by weak adhesive forces. In an electrolyte solution (NaBr, 0.2 mmol litre^{-1}) without a copolymer, only electrostatic repulsion forces corresponding to a quartz surface potential equal to -75 mV acted between the quartz spheres.

The interaction of mica surfaces in solutions of phospholipid, polyglycerol, and their mixtures in triolein has been studied by the Mark-4 device.[70] Ordering of liquid triglyceride molecules results in the bridging of surfaces and gives rise to two barriers related to structural forces. Conversely, the adsorption of polyglycerol induces the appearance of a steric repulsion barrier at a distance of 12 nm. The adsorption of a phospholipid/polyglycerol mixture on the mica surface results in the formation of complexes, which brings about long-range repulsive forces.

The interaction forces between a spherical particle (15 – 25 μm in diameter) of regenerated cellulose and the planar surface of the same polymer were measured by AFM.[71] The long-range repulsion was due to electrostatic forces corresponding to low potentials of regenerated cellulose surfaces. When the surfaces are brought into contact, adhesive forces are detected between the swelled surface layers of cellulose, which represent a viscoelastic gel. The interaction at short distances is reversible. Upon an increase in the electrolyte concentration, the adhesion strength is enhanced.

If the polymer is not adsorbed on the surfaces that confine the interlayer, attractive forces may arise due to the decrease in the osmotic pressure in the solution film between the particles. This effect was observed experimentally by examining the interaction of a glass sphere with a radius of 38 μm with a glass substrate using an atomic force microscope. Both surfaces were precoated with n-octadecyl alcohol layers. The measurements were carried out in solutions of polydimethylsiloxane in cyclohexane.[72] The distance between the surfaces where the attractive forces are manifested is comparable with the radius of gyration of the polymer macromolecule. When the sphere and the plane are brought to a shorter distance, the steric repulsion forces between the overlapping adlayers of n-octadecanol begin to be detectable.

Costello, Luckham and Tadros[73] studied the interaction forces between the mica surfaces with chemically grafted methyl methacrylate/ethylene oxide copolymer using the method of crossed cylinders. In Fig. 4, the dots correspond to experimental values minus the contribution of the electrostatic repulsion forces. The obtained dependences proved to be fully reversible. The continuous curve was constructed using the de Gennes equation[74]

$$\Pi_{st} = \frac{kT}{l^3}\left[\left(\frac{2L}{h}\right)^{9/4} - \left(\frac{h}{2L}\right)^{3/4}\right], \tag{10}$$

where Π_{st} is the steric repulsion force, l is the average distance between the grafting sites of molecules, L is the thickness of the equilibrium grafted layer of the polymer, h is the thickness of the interlayer between the surfaces.

The first term in the right-hand part of Eqn (10) takes into account the effect of the increasing osmotic pressure caused by accumulation of the polymer in the mutually penetrating layers, while the second term corresponds to the elastic forces that tend to restore the initial linear shape of the macromolecules. As can be seen from Fig. 4, the calculated and experimental results are in good agreement with the assumption that $L = 10$ nm.

For polyethylene oxide adsorbed on the mica surface from aqueous solutions, the steric interaction is not reversible, unlike that for grafted polymers.[75] Figure 5 shows the results of measurements of the interaction of crossed mica cylinders in a 0.1 M background solution of KNO_3. In the absence of the polymer, only weak electrostatic repulsion forces can be detected (curve *I*). After keeping the surfaces for 16 h in an aqueous solution of PEO with a molecular mass of 1.6×10^5 (the concentration is 1.5×10^{-4} g ml^{-1}), the repulsive forces follow curve *II*. The same law of variation of the steric forces is obeyed during the repeated bringing together of the surfaces, but only when they have been kept apart for 1 h. Curve *III* corresponds to the repeated compression of the adlayers (bringing the surfaces together), 5 min after the preceding drawing them apart, and to the subsequent fast drawing apart. This short (5 min) period the surfaces are kept far from each other is insufficient for the initial structure of the adsorption layers to be restored. Similar slow rearrangement effects are involved in the case of PEO with a lower molecular weight (1.4×10^4), which is shown by the corresponding

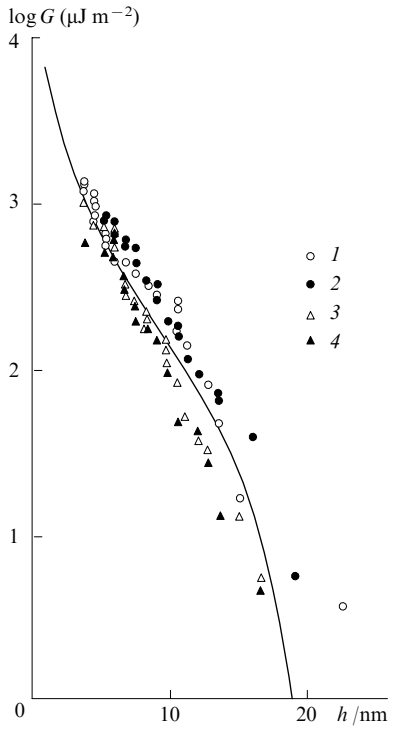


Figure 4. Steric repulsion energy of methyl methacrylate/ethylene oxide copolymer layers grafted to a mica surface in an aqueous 10^{-2} M solution of KNO_3 *vs.* the interlayer thickness.[73]

$$G(h) = \int_h^\infty \Pi_{st}(h)\mathrm{d}h$$

Experimental points: (*1*) the first compression of the grafted copolymer layers, (*2*) the first drawing of the surfaces apart, (*3, 4*) data obtained in the second series of experiments; the curve corresponds to the calculations in terms of the de Gennes theory.[74]

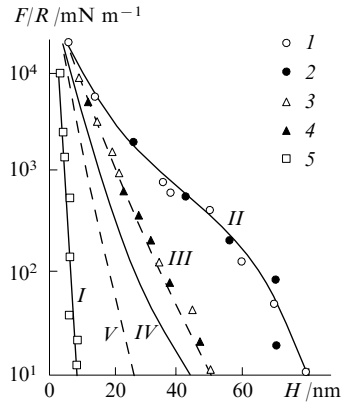


Figure 5. Steric repulsion forces of polyethylene oxide layers adsorbed on mica surfaces *vs.* the distance between the surfaces.[75]
Experimental points: (*1*) the first moving of the surfaces toward each other, (*2*) slow drawing of the surfaces apart after the contact, (*3*) repeated compression of the adlayers 5 min after their preceding separation, (*4*) subsequent fast separation, (*5*) moving of the surfaces toward each other in a 0.1 M solution of KNO_3; (*I – V*) see the text.

curves *IV* and *V*. Thus, the steric forces for grafted and adsorbed polymer molecules are substantially different.

The results of investigations of the interaction forces between various biological objects (cells, lipid bilayers, *etc.*) have been surveyed.[76]

Polyelectrolytes are widely used in modern applied chemistry. This is due to the fact that the charge of the polyelectrolyte chains can be controlled by varying the ion composition and the concentration of the background electrolyte.

The particles of most dispersions used in industry bear a negative charge; therefore, cationic polyelectrolytes (CPE) are used most often for practical purposes. Their influence on the surface interaction was studied by direct measurements of the forces of these interactions in solutions of CPE of various concentrations. It was shown [77] that the electrostatic adsorption of polyethoxylated dodecylamine on a negatively charged mica surface ($\zeta_1 = -105$ mV) takes place at pH < 8 to give a monolayer which shields the surface charge and hydrophobises the surface. This gives rise to molecular attraction forces between the surfaces, which are replaced by steric repulsion forces as the surfaces come closer together. Since the CPE structure contains oxyethyl chains, the hydrophobic attraction forces are not manifested. A decrease in the pH results in reversible structural rearrangement of the adlayer.

Similar results have been obtained for a highly charged cationic polyelectrolyte, poly(2-acryloxyethyl)trimethylammonium chloride with a molecular mass of 1.5×10^6 (see Ref. 78). At a low concentration of the background electrolyte, the molecules of the given CPE were adsorbed on a mica surface as a planar conformation. An increase in the CPE concentration results in gradual shielding of the surface charge of mica and in a decrease in the electrostatic repulsion forces until they completely disappear in the vicinity of the charge reversal point (Fig. 6). The results of measurements (dots) are in good agreement with the results of calculations in terms of the DLVO theory (curves) where the Hamaker constant was taken to be 2.2×10^{-20} J. A further increase in the concentration of poly(2-acryloxyethyl)trimethylammonium chloride induced a slight increase in the adsorption and gave rise to steric forces.

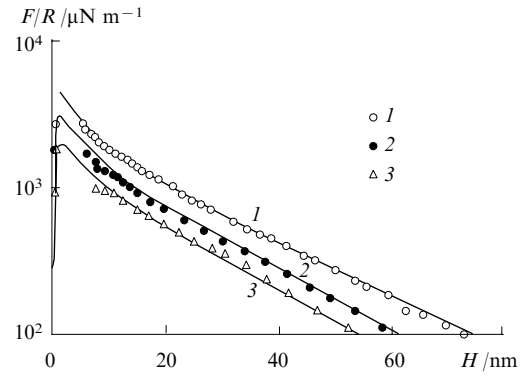


Figure 6. Repulsion force between mica surfaces in aqueous solutions of poly(2-acryloxyethylene)trimethylammonium chloride with a concentration of 1 (*1*), 5 (*2*) and 10 ppm (*3*) containing 0.1 mmol litre^{-1} of KBr *vs.* the distance between them.[78] The curves correspond to the calculation in terms of the DLVO theory.

In dilute solutions of poly(2-vinylpyridine), the interaction forces measured by AFM during moving together of a glass bead and a flat glass substrate also corresponded to analogous forces found in terms of the DLVO theory.[79] However, the adhesion strength at tearing off of the bead was much greater, which is due to the formation of bridging bonds between the surfaces not filled by CPE adlayers with participation of adsorbed CPE molecules. At higher concentrations of CPE and the salt, steric interaction appears and adhesion markedly decreases, which points to a looser state of the adlayer.[79]

It has been reported [80] that at a relatively low concentration of poly(2-vinylpyridine), the AFM-measured interaction remained purely electrostatic. This implies a planar conformation of the

molecules in the adlayer. However, the materials of the bead (quartz) and the substrate (mica) were different; therefore, the surface potentials differed in magnitude, which resulted in switching of the sign of electrostatic forces following a decrease in the solution interlayer thickness. Both the adsorbed CPE molecules and the residual charge of the incompletely shielded substrate contributed to the surface charges formed.

Measurements of the streaming potential of aqueous solutions of the styrene/dimethylaminopropylmaleimide copolymer of various concentrations in thin quartz capillaries with a molecularly smooth surface showed that the isotherm of the electrostatic adsorption of CPE follows the Langmuir equation with an adsorption potential of 25.4 kT (see Ref. 81). This corresponds to the formation of the first layer of planar-oriented molecules. After charge reversal of the solid surface, hydrophobic adsorption of macromolecules takes place to give the second layer. The calculations showed that the hydrophobic adsorption potential is much lower, being equal to 17.7 kT.

Berndt *et al.* [82] have studied the influence on the surface forces of the adsorption of an anionic polyelectrolyte (APE), polystyrenesulfonate with different molecular masses (10^4 to 5×10^5), on positively charged mica surfaces coated by a monolayer of the dioctadecyldimethylammonium cations. For the maximum coverage of the APE monolayer, the interaction forces decrease by an order of magnitude due to the complete neutralisation of the surface charge. The lack of structural forces indicates a planar orientation of the adsorbed APE macromolecules. Thus, these results do not differ qualitatively from those obtained for CPE on negatively charged surfaces.

Using the Mark-4 device, the interaction forces between mica surfaces in sodium polyacrylate solutions, including those containing calcium atoms, have been measured.[83] In the absence of Ca^{2+} ions, no noticeable adsorption of the polymer molecules in mica has been detected. The adsorption started at a $CaCl_2$ concentration higher than 3×10^{-3} mol litre^{-1} due to the formation of bonds between the COO^- groups of the polyelectrolyte and mica with participation of the Ca^{2+} ions. The adhesion strength of the contacting adlayers increased with an increase in the pH.

The same technique was used to measure the interaction forces between mica surfaces in a solution containing 0.2 mg ml^{-1} of proteoglycan (PG) sulfate, which is a part of cellular membranes.[84] The adsorption of PG from a 10^{-4} M solution of NaCl on a hydrophobised mica surface is irreversible. The interaction of the anionic PG adlayers is caused by electrostatic and steric repulsion forces, which show themselves at a distance of less than 10 nm between the surfaces and do not depend on the electrolyte concentration.

The measurement of the interaction forces between the 'brushes' of highly charged diblock copolymer grafted to mica surfaces (hydrophobised by a cationic surfactant) has shown [85] that only electrostatic and short-range steric repulsion can be found between these surfaces. In a salt-free solution, the brushes were straightened under the action of polyelectrolyte counterions. After the addition of a salt, the electrostatic interactions were partially shielded and the polymeric brushes acquired again their flexibility. The region where the interaction is observed depends only slightly on the salt concentration and, when the surfaces move towards each other, it is described adequately by the Pincus scaling theory.[85]

In a number of studies (see, for example, Refs 86–88), osmotic attraction of glass or quartz surfaces in solutions of non-adsorbable polyelectrolytes was detected. The attraction is due to a decrease in the polyelectrolyte concentration in the interlayer between the surfaces whose charge has the same sign as the charge of the polymer.

III. Surface forces in wetting phenomena

1. Wetting films

Wetting films are asymmetrical systems. The surface forces involved in these films can be described using the Derjaguin heterocoagulation theory developed for colloids. Unlike the symmetrical system considered in terms of the DLVO theory, in the wetting films, the field of electrostatic forces is no longer symmetrical as the potentials ψ_1 and ψ_2 of the film surfaces differ in magnitude and, in some cases, also in sign. That is why more diverse combinations of the individual components of the surface forces can be realised in this case. Unlike the symmetrical liquid interlayers between identical surfaces, in the case of wetting films, electrostatic forces often become attractive forces, while dispersion forces are repulsive. The latter is due to the fact that the difference between the dielectric permeabilities $(\varepsilon_2-\varepsilon_3)$ in the equation (5b) for dispersion forces becomes negative in the case of wetting films adjacent to air, because for air, $\varepsilon_2 = 1$.

The thickness h of wetting films formed on planar solid substrates is measured by the method of film-reflected light microinterference or by ellipsometry.[89] The disjoining pressure is specified by the hydrostatic pressure

$$\Pi = \rho g H_h ,$$

where ρ is the density of the liquid, g is the acceleration of gravity and H_h is the difference between the liquid levels in a planar horizontal film and in the vessel it communicates with. By varying the film thickness through specifying different hydrostatic pressures H_h, one can obtain the disjoining pressure isotherms $\Pi(h)$ for wetting films.

It was shown by experiment that the thickness of wetting films of nonpolar liquids is mainly determined by the action of dispersion forces and the isotherm $\Pi(h)$ can be described by Eqn (5a) with the constant A_{130} where subscripts 1, 3 and 0 refer to the substrate, the liquid in the film, and air, respectively.

For volatile liquids, it is possible to obtain the isotherms $\Pi(h)$ by measuring the thickness of polymolecular adsorption films at different relative vapour pressures p/p_s in a preliminary evacuated chamber. In this case, the disjoining pressure in the film is equal to

$$\Pi(h) = -\frac{RT}{\upsilon_m}\ln\frac{p}{p_s}, \qquad (11)$$

where υ_m is the molar volume of the liquid.

Agreement of experimental data with the results of calculation (5a) was obtained for 1–4 nm thick films of alkanes (from pentane to octane) on the surface of quartz.[90] The values of A_{130} thus found were similar for all alkanes — the molecules in the films were mainly oriented parallel to the surface and their different lengths did not affect the result. The possibility of this layered orientation was later confirmed by the Monte Carlo method for n-hexadecane near the gold surface.[91]

Good agreement with the theory of dispersion forces was attained in experiments with cyclohexane, which wets the silicon surface, for thicknesses from 1 to 12 nm.[92] The involvement of other components of surface forces can also be expected in experiments with wetting films of polar liquids.

This is exemplified in Fig. 7, which shows the results of ellipsometric measurements of the thickness of wetting water films on quartz surfaces with different degrees of hydrophilicity. The $h(p/p_s)$ isotherms were obtained for a fully hydroxylated surface of crystalline quartz (curve *1*) and a thermally dehydroxylated surface of the same quartz (curve *4*).[93] The degrees of hydrophilicity of these surfaces are described by water contact angles $\theta = 2-3^\circ$ and 43°, respectively. Isotherms *2* and *3* measured for a polished surface of fused quartz ($\theta = 5-10^\circ$ and 20°, respectively) occupy an intermediate position.[94]

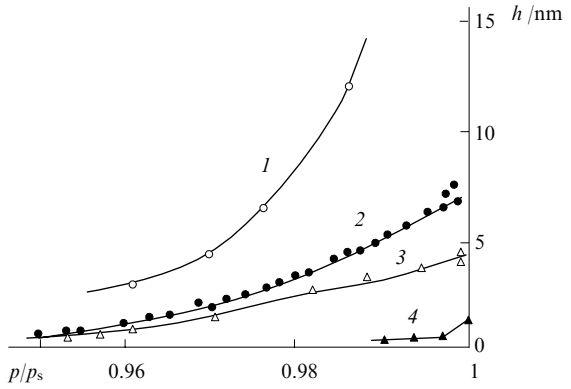


Figure 7. Isotherms of polymolecular adsorption of water vapour on quartz surfaces with different degrees of hydrophilicity. (*1*–*4*) see the text.

The disjoining pressure isotherms obtained for water are consistent with Eqn (8) for structural forces. The influence of electrostatic forces was insignificant, as shown by rough calculations. The involvement of dispersion forces could be expected only for isotherm *4*.

However, it has been shown [95] that isotherms obtained for water films with a thickness of less than 2 nm on mica are not consistent with the isotherms of the theory of dispersion forces. For other polar liquids such as methanol and n-propanol, the isotherms $\Pi(h)$ of thin films (at $p/p_s < 0.8$) are in line with the theory of dispersion forces.[96] However, at a higher vapour pressure, the film thickness exceeds the calculated value due to the additional contribution of electrostatic forces.

Electrolyte solutions form much thicker wetting films, but the region of their existence is limited to a vapour pressure close to saturation. Therefore, the stabilities of these films are studied using the methods described at the beginning of the Section, according to which the disjoining pressure is specified by the hydrostatic pressure (the difference between the liquid levels) or by the capillary pressure of the meniscus.[35, 89] Since electrostatic forces are the longest-range ones, most often, they determine the stability of thick films of aqueous solutions of electrolytes.

The isotherms of the disjoining pressure of the wetting films of aqueous solutions of electrolytes have a characteristic S-shape (Fig. 8). Thick β-films are metastable and at some critical thickness, they break, leaving thinner, thermodynamically stable α-films on the surface. Such films resemble in many aspects the films of pure water on a quartz surface (see Fig. 7).

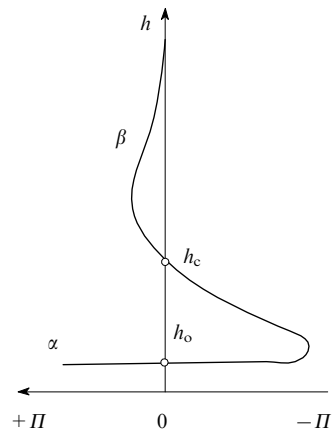


Figure 8. General view of the S-shaped isotherm of disjoining pressure of wetting films including the regions of metastable β-films and thin stable α-films.

The theoretical isotherm for the electrostatic component of the disjoining pressure of water films with the potentials ψ_1 for the boundary with a substrate and ψ_2 for the interface with air has the form

$$\Pi_e(h) = \left(\frac{RTc}{\mathrm{sh}^2(\kappa h)}\right)[2\Phi_1\Phi_2\mathrm{ch}(\kappa h) - (\Phi_1)^2 - (\Phi_2)^2], \qquad (12)$$

where c is the concentration of the solution, mol ml^{-1}, $\Phi = ze\psi/kT$ is the dimensionless potential of the interface.

Using Eqn (12), one can obtain a quantitative interpretation of the upper section of the S-shaped isotherm shown in Fig. 8 and explain the possibility of rupture of β-films upon thinning, namely, switching from the electrostatic repulsion forces, which maintain the stability of thick β-films, to electrostatic attraction forces takes place as the film thickness reaches the critical value

$$h_c = \kappa^{-1}\ln\left(\frac{\psi_1}{\psi_2}\right). \qquad (13)$$

The dependence of the thickness of wetting films on a planar quartz surface on the concentration and pH of an electrolyte (KCl) solution at a constant ionic strength equal to 10^{-3} mol litre^{-1} has been studied by microinterference.[97] The experimental data obtained for thicknesses of about 100 nm were consistent with theoretical results provided that the potentials ψ_1 and ψ_2 of the film surfaces were constant. The potentials ψ_1 and ψ_2 known from electrokinetic measurements and data for foam films were used. According to the theory, the loss of stability occurs at pH < 8 and at an electrolyte concentration of $> 10^{-3}$ mol litre^{-1}. After rupture of the β-films, drops of the bulk solution forming contact angles of 10–25° (which correspond to incomplete wetting) with the remaining thin α-film were left on the surface.

The known analytical solutions for electrostatic forces were obtained for two limiting cases, namely, constant potentials (ψ = const) or constant charges (σ = const) for both film surfaces upon the change in the film thickness. McCormack *et al.*[98] considered cases where different boundary conditions may be fulfilled on the interfaces of the film. In particular, for a constant potential of the surface of the solid substrate (ψ_1 = const) and a constant charge (σ_2 = const) of the film–gas interface, the expression for the electrostatic component of the disjoining pressure assumes the form [94]

$$\Pi(h) = nkT\left[\frac{\Phi_1}{\mathrm{ch}(\kappa h)} + \Phi_2\mathrm{th}(\kappa h)\right]^2 - \Phi_{2\infty}^2, \qquad (14)$$

where n is the concentration of ions; the potential ψ_1 is taken to be independent of the film thickness, and the $\psi_{2\infty}$ potential is taken for $h \to \infty$. As the film thickness decreases, the ψ_2 values start to depend on the thickness, which corresponds to a constant charge σ_2 of the film–gas interface.

The film rupture under the conditions described above takes place at a critical thickness h_c, which can be determined from Eqn (14) using the known criterion for film stability, $d\Pi/dh = 0$

$$\mathrm{sh}(\kappa h_c) = \frac{\Phi_{2\infty}}{\Phi_1}. \qquad (15)$$

This expression has been used [99] to explain the stability of 45-nm films of a 10^{-4} M solution of KCl formed between the surface of a thin quartz capillary (r = 4.5 μm) and a gas bubble.

A clear idea of the properties of wetting films of aqueous solutions of electrolytes at different boundary conditions can be gained from Fig. 9. Here curve *1* is the disjoining pressure isotherm calculated from Eqn (14) with dimensionless surface potentials $\Phi_1 = 8$ and $\Phi_{2\infty} = 2$; for comparison, the Figure shows isotherms *2* and *3* calculated for identical boundary conditions at both interfaces of the film (σ = const or ψ = const, respectively). The Figure demonstrates how different electrostatic boundary conditions influence the thickness and stability of wetting films of aqueous solutions of electrolytes. When the charge is constant on both surfaces of the film (curve *2*), the

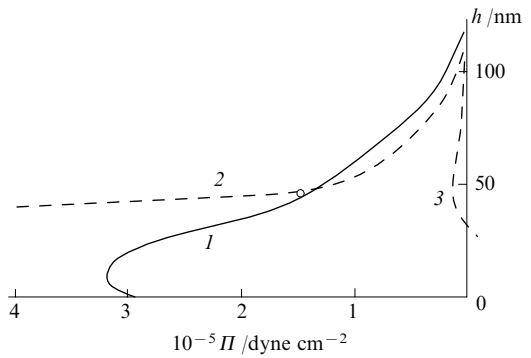


Figure 9. Disjoining pressure isotherms of wetting films calculated for various boundary conditions:
(*1*–*3*) see the text.

films remain stable over a broad range of disjoining pressures, while in the case of constant potentials (curve *3*), the films lose stability even at low pressures when the film thickness approaches the critical value [see Eqn (13)].

The presence of surfactants in aqueous solutions influences considerably the thickness and stability of wetting films. Nonionic surfactants influence the degree of hydrophilicity of the film surfaces; this can change the magnitude and the sign of the short-range structural forces. The influence of the adsorption of ionic surfactants is more pronounced, as it changes the magnitude and the sign of electrostatic long-range forces.

Gee *et al.*[93] have measured the thickness of wetting films on a polished quartz surface as a function of the concentration of aqueous solutions of CTAB by ellipsometry and microinterference. Unlike the preceding studies, the potentials of the film surface ψ_1 and ψ_2 were measured by independent methods.[95] The measurements showed that in the region of $c_{\mathrm{CTAB}} < 10^{-7}$ mol litre^{-1}, the films were metastable, because the surface potentials, though having like signs, still differed in magnitude. On further increase in the surfactant concentration, the films lost stability, and the contact angles they formed with the substrate had a maximum ($\theta \approx 50-60^{\circ}$) at $c_{\mathrm{CTAB}} = 10^{-5}$ mol litre^{-1}. The film stability was restored on approaching the CMC ($c_{\mathrm{CTAB}} \approx 10^{-3}$ mol litre^{-1}) where both film surfaces acquired equal positive charges. The observation of the charge reversal for quartz surfaces in solutions of CTAB has been used, in particular, to evaluate the efficiency of flotation.[100]

The rupture of wetting films of aqueous solutions of another cationic surfactant, dodecylamine, has been observed at concentrations below the CMC.[101] The effect of an anionic surfactant, sodium dodecyl sulfate, on the stability of water wetting films is less pronounced, because its presence increases only slightly the negative charge of the quartz surface.[102] Upon adsorption of sodium dodecyl sulfate, the negative charge of the second surface of the film also increases; therefore, film stability is enhanced.

Comparative analysis of the results obtained for wetting and foam films of surfactant solutions has provided an explanation for the difference in their stability mechanisms.[103, 104]

The same experimental methods were employed to study films of aqueous solutions occurring between a solid surface and a liquid immiscible with water (*e.g.*, oil).[105, 106] Such systems can model emulsion films.

The thickness of a water film formed between quartz and silicone oil (with a molecular mass of 2400) was $\approx 50-60$ nm at a concentration of the background electrolyte (KCl) of 10^{-4} mol litre^{-1} (see Ref. 105); this was much smaller than the thickness of a wetting film adjacent to air. Similar results have been obtained for films of aqueous solutions of CTAB with a concentration from 4×10^{-4} to 10^{-3} mol litre^{-1} in contact with silicon oil or tetradecane. Under these conditions, either an oil-in-water or a water-in-oil emulsion is formed in quartz capillaries, depending on the direction of movement of the oil–water meniscus.[107]

Stable water films were also observed between quartz and xylene,[105] in particular, with solutions containing nonionic surfactants.[106]

Let us consider how the presence of a polymer in the solution influences the wetting film stability. A substantial additional contribution can be expected from steric repulsion forces, caused by the deformation of the polymer adsorption layers when they are brought into contact. The radius of action of these forces depends on the length of the macromolecule and its conformation in the adsorbed state.

Gasanov *et al.*[108] have obtained disjoining pressure isotherms for wetting films of aqueous solutions of polyethylene oxide with a molecular mass of 6×10^5 on a planar quartz surface. However, the thickness of the adsorption layer of the polymer on quartz (20 nm) was much smaller than the thickness of the films studied (50–100 nm). Therefore, the role of the polymer was only to decrease somewhat the film thickness (by 5–10 nm) due to shielding of a part of the surface charge of quartz by the macromolecules adsorbed due to the formation of hydrogen bonds with the surface hydroxy groups.

In wetting films of aqueous solutions of the triblock copolymer F108 with a molecular mass of 1.4×10^4 whose molecules are composed of the central hydrophobic polypropylene oxide block and two terminal hydrophilic PEO blocks, adsorption took place on both interfaces.[109] As the adsorption layers approached each other and finally overlapped, stable (due to steric repulsion forces) 30–40-nm thick films were formed.

The use of cationic polyelectrolytes also allows one to stabilise wetting films. In solutions of the highly charged styrene/dimethylaminopropylmaleimide polymers, the major effect is due to electrostatic forces.[110] In this case, the stability of wetting films can be controlled by varying the composition and chain length of the polymer and the charge and conformation of molecules in solutions with different ion compositions.

2. Wetting control

The use of disjoining pressure isotherms of wetting films makes it possible to estimate the contact angles θ formed by liquids on solid substrates. The corresponding expression is derived from combination of the Frumkin–Derjaguin theory of free surface energy γ_{sv} of a solid substrate coated by an equilibrium wetting film with the thickness h_0,

$$\gamma_{\mathrm{sv}} = \gamma_{\mathrm{sl}} + \gamma_{\mathrm{lv}} + G(h_0), \tag{16}$$

where $G(h_0)$ is the free Gibbs energy of the equilibrium film

$$G(h_0) = \int_{h_0}^{\infty} \Pi(h)\mathrm{d}h,$$

on the one hand, and the known Young equation

$$\gamma_{\mathrm{lv}} \cos\theta = \gamma_{\mathrm{sv}} - \gamma_{\mathrm{sl}}, \tag{17}$$

where γ_{lv} is the surface tension of the liquid, γ_{sl} is the free energy of the solid–liquid interface, on the other hand. By combining the two equations, we get [110–112]

$$\cos\theta = 1 + \frac{G(h_0)}{\gamma_{\mathrm{sl}}}. \tag{18}$$

The equilibrium film thickness h_0 can be found by solving the equation of the overall isotherm, which includes the dispersion, electrostatic, structural and steric forces

$$\Pi(h) = \Pi_{\mathrm{m}}(h) + \Pi_{\mathrm{e}}(h) + \Pi_{\mathrm{s}}(h) + \Pi_{\mathrm{ster}}(h) = 0\,. \tag{19}$$

The equilibrium film thickness h_0 is determined as the smallest root of Eqn (19), which corresponds to intersection of the isotherm with the axis of thicknesses (see Fig. 8). This method of calculation can be used for macroscopic drops and meniscuses

where the equilibrium vapour pressure above the film is close to the saturation pressure.

Examples of calculations of the dependences of contact angles on the magnitude and sign of the surface charge, the Hamaker constants and the structural repulsion and hydrophobic attraction forces have been reported.[111–113] Comparison of the results of calculations with experimental data showed that the effect of hydrophilic repulsion forces can be detected at contact angles of $\theta < 15-20^\circ$, while the effect of hydrophobic attraction forces, at $\theta > 50-60^\circ$. In the intermediate region of θ values, wetting can be described using the DLVO theory.

The proposed calculation methods can be used to predict wetting and to select the optimal composition of solutions that ensure the required process conditions, for example, for flotation, dust extraction and capillary impregnation.

This work was written with partial financial support of the Russian Foundation for Basic Research (Project No. 01-03-32112).

References

1. B V Derjaguin, N V Churaev, V M Muller *Poverkhnostnye Sily* (Surface Forces) (Moscow: Nauka, 1987)
2. W B Russel, D A Saville, W R Schowalter *Colloidal Dispersions* (Cambridge: Cambridge University Press, 1989)
3. B V Derjaguin *Kolloid. Zh.* **17** 207 (1955)
4. B V Derjaguin *Zh. Fiz. Khim.* **6** 1306 (1935)
5. L N McCartney, S Levine *J. Colloid Interface Sci.* **30** 345 (1969)
6. doi D J Mitchell, B V Ninham *J. Chem. Phys.* **56** 1117 (1972)
7. J E Kiefer, V A Parsegian, G H Weiss *J. Colloid Interface Sci.* **67** 140 (1978)
8. doi J Chen, A Anandarajan *J. Colloid Interface Sci.* **180** 519 (1996)
9. L Beloni, O Spalla *Ber. Bunsen-Ges. Phys. Chem.* **100** 905 (1996)
10. E M Lifshits *Zh. Eksp. Teor. Fiz.* **29** 94 (1955)
11. I E Dzyaloshinskii, E M Lifshits, L P Pitaevskii *Zh. Eksp. Teor. Fiz.* **37** 229 (1959)
12. H C Hamaker *Physica* **4** 1058 (1937)
13. doi H B Casimir, D Polder *Phys. Rev.*, **73** 36 (1948)
14. doi J Visser *Adv. Colloid Interface Sci.* **3** 331 (1972)
15. doi D B Hough, L R White *Adv. Colloid Interface Sci.* **14** 3 (1980)
16. M K Chaudhury, R J Good *J. Colloid Interface Sci.* **94** 292 (1983)
17. Ya I Rabinovich, N V Churaev *Kolloid. Zh.* **46** 69 (1984) [a]
18. doi R R Fernandez-Varea, R Garcia-Molina *J. Colloid Interface Sci.* **231** 394 (2000)
19. doi R R Dagastine, D C Prieve, L R White *J. Colloid Interface Sci.* **231** 351 (2000)
20. doi L Bergstrom *Adv. Colloid Interface Sci.* **70** 125 (1997)
21. J N Israelachvili *Intermolecular and Surface Forces* (New York: Academic Press, 1985)
22. D Y C Chen, R M Pashley, R L White *J. Colloid Interface Sci.* **77** 283 (1980)
23. doi S S Dukhin *Adv. Colloid Interface Sci.* **44** 1 (1993)
24. R Kjellander *Ber. Bunsen-Ges. Phys. Chem.* **100** 894 (1996)
25. doi G Toikka, R A Hayes *J. Colloid Interface Sci.* **191** 102 (1997)
26. doi I Larson, C J Drummond, D Y C Chen, F Grieser *Langmuir* **13** 2109 (1997)
27. doi B V Zhmud, A Meurk, L Bergstrom *J. Colloid Interface Sci.* **207** 332 (1998)
28. doi O Teschke, E F de Souza, G Ceotto *Langmuir* **15** 4935 (1999)
29. S S Dukhin, J Lyklema *Kolloid. Zh.* **53** 466 (1991) [a]
30. doi A M Islam, B Z Chowdhry, M J Snowden *Adv. Colloid Interface Sci.* **62** 109 (1995)
31. doi R G Horn, D T Smith *J. Non-Cryst. Solids* **120** 72 (1990)
32. Q Du, E Freysz, Y R Chen *Science* **264** 826 (1994)
33. N V Churaev *Kolloid. Zh.* **58** 725 (1996) [a]
34. G A Martynov *Zh. Fiz. Khim.* **73** 1744 (1999) [b]
35. N V Churaev *Fizikokhimiya Protsessov Massoperenosa v Poristykh Telakh* (Physical Chemistry of Mass Transfer Processes in Porous Solids) (Moscow: Khimiya, 1990)
36. doi A A Kornyshev, S Leikin *Phys. Rev. A* **40** 6431 (1989)
37. doi V S Mitlin, M M Sharma *J. Colloid Interface Sci.* **157** 447 (1993)
38. doi A Trokhimchuk, D Henderson, D T Wasan *J. Colloid Interface Sci.* **210** 320 (1999)
39. R Winkler, A Gerstmair, P Reineker, N Matsuda, D Y Yoon *Int. J. Quantum Chem.* **52** 437 (1994)
40. J Forsman, B Jonsson, C E Woodward *J. Phys. Chem. B* **101** 4253 (1997)
41. doi M Hato *J. Phys. Chem.* **100** 18530 (1996)
42. doi H K Christenson, P M Claesson *Adv. Colloid Interface Sci.* **91** 391 (2001)
43. W A Ducker, Z Xu, J N Israelachvili *Langmuir* **10** 3279 (1994)
44. E Ruckenstein, N Churaev *J. Colloid Interface Sci.* **147** 535 (1991)
45. doi V S J Craig, B W Ninham, R M Pashley *Langmuir* **15** 1562 (1999)
46. L Meagher, V S Craig *Langmuir* **10** 2736 (1994)
47. doi N Ishida, M Sakamoto, M Miyahara, K Higashitani *Langmuir* **16** 5681 (2000)
48. doi N Ishida, T Inoue, M Miyahara, K Higashitani *Langmuir* **16** 6377 (2000)
49. doi R F Considine, C J Drummond *Langmuir* **16** 631 (2000)
50. doi Y Gu, D Li *J. Colloid Interface Sci.* **226** 328 (2000)
51. Z M Zorin, T Kolarov, N E Esipova, D Platikanov, I P Sergeeva *Kolloid. Zh.* **52** 666 (1990) [a]
52. E D Shchukin, A V Pertsov, E A Amelina *Kolloidnaya Khimiya* (Colloid Chemistry) (Moscow: Moscow State University, 1982) p. 176
53. I Larson, C J Drummond, D Y C Chan, F Grieser *J. Am. Chem. Soc.* **115** 11885 (1993)
54. Y Q Li, N J Tao, J Pan, A A Garsia, S M Lindsay *Langmuir* **9** 637 (1993)
55. D T Atkins, R M Pashley *Langmuir* **9** 2232 (1993)
56. doi A Carambassis, M W Rutland *Langmuir* **15** 5584 (1999)
57. doi V V Yaminsky, B W Ninham, R M Pashley *Langmuir* **12** 3223 (1998)
58. doi S Bhattacharjee, C-H Ko, M Elimelech *Langmuir* **14** 3365 (1998)
59. E Veeramasunneni, Y Hu, M R Yalamanchili, J D Miller *Langmuir* **188** 473 (1997)
60. I P Sergeeva, V M Muller, M A Zakharova, V D Sobolev, N V Churaev *Kolloid. Zh.* **57** 400 (1995) [a]
61. V M Muller, I P Sergeeva, N V Churaev *Kolloid. Zh.* **57** 368 (1995) [a]
62. doi P Kekicheff, H K Christenson, B W Ninham *Colloids Surf.* **40** 31 (1989)
63. I P Sergeeva, V D Sobolev, N V Churaev, H-J Jakobasch, P Veidenkhammer, F I Shmitt *Kolloid. Zh.* **60** 645 (1998) [a]
64. doi W A Ducker, E J Wanless *Langmuir* **15** 160 (1999)
65. M W Ruthland, J L Parker *Langmuir* **10** 1110 (1994)
66. Z M Zorin, E K Gasanov, N E Esipova, I N Kornil'ev *Kolloid. Zh.* **53** 25 (1995) [a]
67. E N Nikologorskaya, V A Kosaikin, N V Churaev *Kolloid. Zh.* **52** 502 (1990) [a]
68. I Pezron, E Pezron, P M Claesson, M Malmsten *Langmuir* **7** 2248 (1991)
69. doi K Eskilsson, B W Ninham, F Tiberg, V V Yaminsky *Langmuir* **14** 7287 (1998)
70. doi A Dedinaite, B Campbell *Langmuir* **16** 2248 (2000)
71. doi S Zauscher, D J Klingenberg *J. Colloid Interface Sci.* **229** 457 (2000)
72. doi A Milling, S Biggs *J. Colloid Interface Sci.* **170** 604 (1995)
73. doi B A Costello, P F Luckham, Th F Tadros *Colloids Surf.* **34** 301 (1989)
74. doi P G de Gennes *Adv. Colloid Interface Sci.* **27** 189 (1987)
75. J Klein, P Luckham *Nature (London)* **300** 429 (1982)
76. doi P F Luckham, P G Hartley *Adv. Colloid Interface Sci.* **49** 341 (1994)
77. doi A Waltermo, M Sjoberg, B Arnhede, P M Claesson *J. Colloid Interface Sci.* **156** 365 (1993)
78. doi M A G Dahlgren, P M Claesson, R Audebert *J. Colloid Interface Sci.* **166** 343 (1994)
79. doi S Biggs, A D Proud *Langmuir* **13** 7202 (1997)
80. doi P G Hartley, P J Scales *Langmuir* **14** 6948 1998
81. I P Sergeeva, T B Ermakova, V D Sobolev, N V Churaev *Kolloid. Zh.* **65** 662 (2003) [a]
82. P Berndt, K Kurihara, T Kunitake *Langmuir* **8** 2486 (1992)

83. J M Berg, P M Claesson, R D Neuman *J. Colloid Interface Sci.*, **161** 182 (1993)
84. M Malmsten, P Claesson, G Siegel *Langmuir* **10** 1274 (1994)
85. T Abraham, S Giasson, J F Gohy, R Jerome *Langmuir* **16** 4286 (2000)
86. E S Pagac, R D Tilton, C Prieve *Langmuir* **14** 5106 (1998)
87. A J Milling, K Kendall *Langmuir* **16** 5106 (2000)
88. S Biggs, J L Burns, Y-de Yan, G J Jameson *Langmuir* **16** 9242 (2000)
89. B V Derjaguin, N V Churaev *Smachivayushchie Plenki* (Wetting Films) (Moscow: Nauka, 1984)
90. M L Gee, T W Healy, L R White *J. Colloid Interface Sci.* **131** 19 (1989)
91. S Balasubramanian, M L Klein, J I Siepman *J. Chem. Phys.* **103** 3184 (1995)
92. I M Tidswell, T A Rabedeau, P S Pershau *Phys. Rev. B* **49** 10869 (1991)
93. M L Gee, T W Healy, L R White *J. Colloid Interface Sci.* **140** 450 (1990)
94. N V Churaev *Kolloid. Zh.* **62** 581 (2000) [a]
95. D Beaglehole, E Z Radzinska, B W Ninham, H K Christenson *Phys. Rev. Lett.* **66** 2084 (1991)
96. M L Gee, T W Healy, L R White *J. Colloid Interface Sci.* **133** 514 (1989)
97. I N Kornil'ev, Z M Zorin, N V Churaev *Kolloid. Zh.* **46** 892 (1984) [a]
98. D McCormack, S L Carnie, D Y C Chan *J. Colloid Interface Sci.* **169** 177 (1995)
99. A P Ershov, Z M Zorin, V D Sobolev, N V Churaev *Kolloid. Zh.* **63** 179 (2001) [a]
100. L Alexandrova, R J Pugh, F Tiberg, L Grigorov *Langmuir* **15** 7464 (1999)
101. P Somasundaran, S Simpson, I Ivanov, R K Jain, D Sarkar *Langmuir* **15** 7658 (1999)
102. Z M Zorin, E K Gasanov, N E Esipova, I N Kornil'ev *Kolloid. Zh.* **53** 25 (1991) [a]
103. T Kolarov, R Yankov, N E Esipova, D Exerova, Z Zorin *Colloid Polym. Sci.* **271** 519 (1993)
104. D Exerova, N V Churaev, T Kolarov, N E Esipova, N Panchev, Z M Zorin *Adv. Colloid Interface Sci.* **104** 1 (2003)
105. N P Hankins, J A Haynes, S D Lubetkin, in *Chemical Colloids and Interfaces in Oil Production* (Paris: Technip, 1992) p. 59
106. B P Binks, W S Cho, P D I Fletcher *Langmuir* **13** 7180 (1997)
107. A P Ershov, N E Esipova, M A Zakharova, Z M Zorin, G A Iskandyar, E A Madzharova, I P Sergeeva, V D Sobolev, T F Svitova, N V Churaev *Kolloid. Zh.* **56** 53 (1994) [a]
108. E K Gasanov, I P Sergeeva, V D Sobolev, Z M Zorin, N V Churaev *Kolloid. Zh.* **53** 617 (1991) [a]
109. N E Esipova, S V Itskov, N V Churaev *Kolloid. Zh.* **64** 775 (2002) [a]
110. I P Sergeeva, T B Ermakova, N V Churaev, K Grundke, O Yudin *Kolloid. Zh.* **64** 531 (2002) [a]
111. N V Churaev *Kolloid. Zh.* **56** 707 (1994) [a]
112. N V Churaev, V D Sobolev *Kolloid. Zh.* **57** 888 (1995) [a]
113. N V Churaev, V D Sobolev *Kolloid. Zh.* **62** 278 (2000) [a]

[a] — *Colloid. J. (Engl. Transl.)*
[b] — *Russ. J. Phys. Chem. (Engl. Transl.)*